optica

Grayscale transparent metasurface holograms

Lei Wang,[1] Sergey Kruk,[1,*] Hanzhi Tang,[1,2] Tao Li,[2] Ivan Kravchenko,[3] Dragomir N. Neshev,[1] and Yuri S. Kivshar[1]

[1]Nonlinear Physics Centre, Research School of Physics and Engineering, Australian National University, Canberra ACT 2601, Australia
[2]National Laboratory of Solid State Microstructures, College of Engineering and Applied Sciences, Nanjing University, Nanjing 210093, China
[3]Oak Ridge National Laboratory, Oak Ridge, Tennessee 37831, USA
*Corresponding author: Sergey. Kruk@anu.edu.au

Received 22 November 2016; revised 1 December 2016; accepted 4 December 2016 (Doc. ID 281219); published 16 December 2016

We demonstrate transparent metaholograms based on silicon metasurfaces that allow high-resolution grayscale images to be encoded. The holograms feature the highest diffraction and transmission efficiencies, and operate over a broad spectral range.

OCIS codes: (160.3918) Metamaterials; (090.0090) Holography; (160.4236) Nanomaterials.

https://doi.org/10.1364/OPTICA.3.001504

Metasurfaces are ultra-thin patterned structures that emerged recently as planar metadevices [1] capable of reshaping and controlling incident light. They are composed of resonant subwavelength elements that are distributed spatially across a surface. Due to resonant scattering, each element can alter the phase, amplitude, and polarization of the incoming light. Many designs and functionalities of metasurfaces suggested so far are based largely on plasmonic planar structures [2]; however, most of these metasurfaces demonstrate low efficiencies in transmission due to losses in their metallic components. In contrast, *all-dielectric resonant nanophotonic structures* [3] avoid absorption losses and can drastically enhance the overall efficiency [4–9], especially in the transmission regime. Recently, we have seen a number of demonstrations of all-dielectric metasurfaces with ever-increasing transmission efficiencies, in both the near-infrared [4–8] and visible [9] spectral ranges, including full phase and polarization control. This makes dielectric metasurfaces a promising novel platform for flat optical devices, such as waveplates, Q-plates, lenses, and holograms.

Holograms, in particular, showcase a potential of the metasurface platform, as they rely on complex wavefront engineering. The field of holography has gone through several transformations triggered by new technologies. While originally, holographic methods were applied in electron microscopy [10], the advent of lasers brought their practical implementation in optics. The development of computer-generated holography has further advanced this field. Today, we witness the next revolutionary step in holographic optics driven by the enormous progress in our ability to structure materials at the nanoscale [9,11–15]. This in particular, enables a new way to create highly efficient holograms with single-step patterning.

Here, we design and realize experimentally grayscale metaholograms with superior transmission properties. We employ the concept of the multi-resonant response based on the generalized Huygens' principle [8], which provides a clear procedure to suppress the backward scattering for multiple wavelengths, allowing forward-light propagation with almost no reflection. We design different types of holograms composed of subdiffraction lattices of silicon nanopillars, each supporting several electric and magnetic Mie resonances [3]. The nanopillars feature a size-dependant phase delay, which allows us to achieve 2π phase variations across the hologram with over 2π variation across the operational spectral bandwidth. Based on this principle, we fabricate different metaholograms and demonstrate experimentally diffraction efficiencies over 99% with transmission efficiencies over 90%.

We use CST Microwave Studio to design the metaholograms. We employ a set of 36 different silicon nanopillars with 865 nm height and radii ranging from 79 to 212 nm, arranged in a square lattice with a 750 nm period. Each nanopillar serves as a subdiffractional pixel for the hologram. We design the holograms with the band-limited angular spectrum method and the Gerchberg–Saxton algorithm. Our holograms have sizes of 0.75 mm and produce 5 mm large images at a distance of 10 mm. To fabricate the metasurfaces, we deposit poly-silicon on a silica wafer with low-pressure chemical vapor deposition. Electron beam lithography defines the geometry of the nanopillars, and reactive ion etching translates the geometry into silicon.

Figure 1(a) shows the electron microscope images of one of the fabricated metaholograms, and Fig. 1(b) shows its visible dark-field optical microscope image. This image resembles a layout of the designed phase mask, since nanopillars of different sizes scatter different visible wavelengths. Figure 1(c) show the calculated images. We experimentally observe holographic images on an infrared camera by illuminating the samples with a collimated laser beam of a matching size. Figure 1(d) shows the experimental images reconstructed from two holograms under illumination with a wavelength of 1600 nm.

Next, we study the operational bandwidths of the metaholograms in terms of their transmission and diffraction efficiencies. The diffraction efficiency is defined as the power concentrated in the holographic image referenced to the total power transmitted by the hologram, and the bandwidth is defined as the spectral full

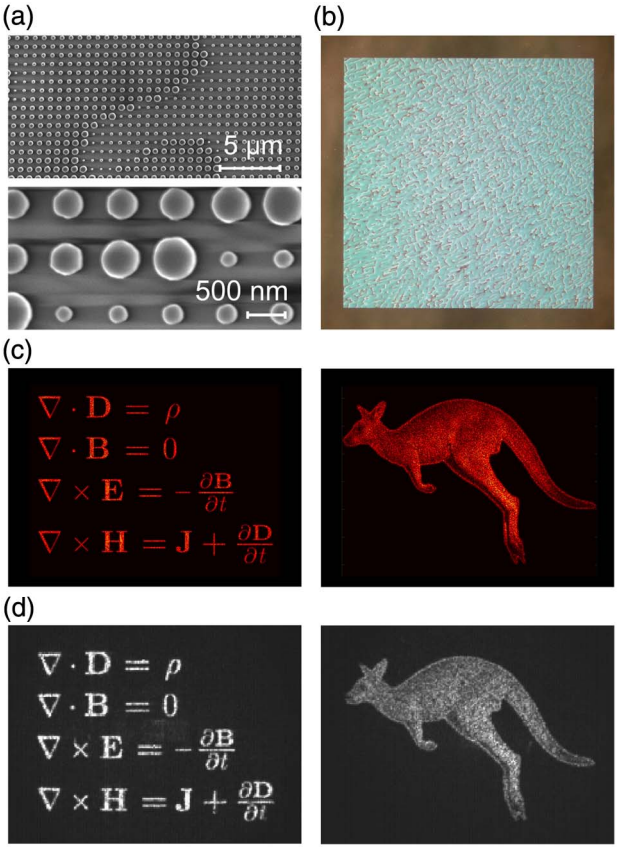

Fig. 1. Examples of fabricated metaholograms. (a) Scanning electron microscope images of fabricated metaholograms. (b) Visible light dark-field microscope image of a holographic metasurface. (c) Theoretical and (d) experimental holographic images from two holograms at a 1600 nm wavelength.

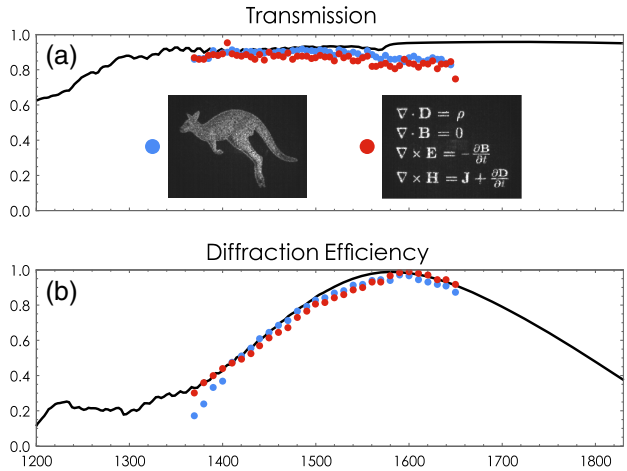

Fig. 2. Superior performance of metaholograms. (a) Transmission and (b) diffraction efficiencies of two holograms (curves: theory, dots: experimental data). Insets show holographic images at different wavelengths.

width at half-maximum. We use lasers tunable in the spectral range from 1360–1650 nm. We also numerically study the efficiency spectra with CST Microwave Studio. Figures 2(a) and 2(b) show the experimental and numerical spectra for both the transmission and diffraction efficiencies.

Our metaholograms produce grayscale high-resolution images and transmit over 90% of light with a diffraction efficiency over 99% at a 1600 nm wavelength. The operation spectral bandwidth is 375 nm. This is the highest efficiency of any metaholograms demonstrated to date reproducing grayscale images over a broad spectral range. The design approach is applicable to other materials with high refractive index, such as Ge, GaAs, TiO_2, diamond, etc. The operation range is scalable to other wavelengths and, in particular, to the visible spectrum.

Funding. Australian Research Council (ARC).

Acknowledgment. We acknowledge support from the Chinese Scholarship Council. We thank B. Luther-Davies for providing the tunable lasers. Part of this research was conducted at the Center for Nanophase Materials Sciences, which is a DOE Office of Science User Facility.

REFERENCES

1. N. I. Zheludev and Y. S. Kivshar, Nat. Mater. **11**, 917 (2012).
2. N. Yu and F. Capasso, Nat. Mater. **13**, 139 (2014).
3. A. I. Kuznetsov, A. E. Miroshnichenko, M. L. Brongersma, Y. S. Kivshar, and B. Luk'yanchuk, Science **354**, aag2472 (2016).
4. P. Lalanne, S. Astilean, P. Chavel, E. Cambril, and H. Launois, Opt. Lett. **23**, 1081 (1998).
5. D. Lin, P. Fan, E. Hasman, and M. L. Brongersma, Science **345**, 298 (2014).
6. M. Decker, I. Staude, M. Falkner, J. Dominguez, D. N. Neshev, I. Brener, T. Pertsch, and Y. S. Kivshar, Adv. Opt. Mater. **3**, 813 (2015).
7. A. Arbabi, Y. Horie, M. Bagheri, and A. Faraon, Nat. Nanotechnol. **10**, 937 (2015).
8. S. Kruk, B. Hopkins, I. I. Kravchenko, A. Miroshnichenko, D. N. Neshev, and Y. S. Kivshar, APL Photon. **1**, 030801 (2016).
9. M. Khorasaninejad, A. Ambrosio, P. Kanhaiya, and F. Capasso, Sci. Adv. **2**, e1501258 (2016).
10. D. Gabor, Nature **161**, 777 (1948).
11. G. Zheng, H. Mühlenbernd, M. Kenney, G. Li, T. Zentgraf, and S. Zhang, Nat. Nanotechnol. **10**, 308 (2015).
12. D. Wen, F. Yue, G. Li, G. Zheng, K. Chan, S. Chen, M. Chen, K. F. Li, P. W. H. Wong, K. W. Cheah, E. Y. B. Pun, S. Zhang, and X. Chen, Nat. Commun. **6**, 8241 (2015).
13. B. Wang, F. Dong, Q.-T. Li, D. Yang, C. Sun, J. Chen, Z. Song, L. Xu, W. Chu, Y.-F. Xiao, Q. Gong, and Y. Li, Nano Lett. **16**, 5235 (2016).
14. K. E. Chong, L. Wang, I. Staude, A. R. James, J. Dominguez, S. Liu, G. S. Subramania, M. Decker, D. N. Neshev, I. Brener, and Y. S. Kivshar, ACS Photon. **3**, 514 (2016).
15. X. Li, L. Chen, Y. Li, X. Zhang, M. Pu, Z. Zhao, X. Ma, Y. Wang, M. Hong, and X. Luo, Sci. Adv. **2**, e1601102 (2016).